Threonine-89 Participates in the Active Site of Bacteriorhodopsin: Evidence for a Role in Color Regulation and Schiff Base Proton Transfer†

Terence S. Russell,‡ Matthew Coleman,‡ Parshuram Rath, Anders Nilsson,§ and Kenneth J. Rothschild*

Physics Department and Molecular Biophysics Laboratory, Boston University, Boston, Massachusetts 02215

Received February 6, 1997; Revised Manuscript Received April 14, 1997⊗

ABSTRACT: Bacteriorhodopsin (bR) functions as a light-driven proton pump in the purple membrane of *Halobacterium salinarium*. A major feature of bR is the existence of an active site which includes a retinylidene Schiff base and amino acid residues Asp-85, Asp-212, and Arg-82. This active site participates in proton transfers and regulates the visible absorption of bacteriorhodopsin and its photointermediates. In this work we find evidence that Thr-89 also participates in this active site. The substitution Thr-89 → Asn (T89N) results in changes in the properties of the *all-trans* retinylidene chromophore of light-adapted bR including a redshift of the visible λ_{max} and a downshift in C═N and C═C stretch frequencies. Changes are also found in the M and N intermediates of the T89N photocycle including shifts in λ_{max}, a downshift of the Asp-85 carboxylic acid C═O stretch frequency by 10 cm^{-1}, and a 3−5-fold decrease in the rate of formation of the M intermediate. In contrast, the properties of the 13-*cis* retinylidene chromophore of dark-adapted T89N as well as the K and L intermediates of the T89N photocycle are similar to the wild-type bacteriorhodopsin. These results are consistent with an interaction of the hydroxyl group of Thr-89 with the protonated Schiff base of light-adapted bR and possibly the N intermediate but not the 13-*cis* chromophore of dark-adapted bR or the K and L intermediates. Thr-89 also appears to influence the rate of Schiff base proton transfer to Asp-85 during formation of the M intermediate, possibly through an interaction with Asp-85. In contrast, the hydroxyl group of Thr-89 is not obligatory for proton transfer from Asp-96 to the Schiff base during formation of the N intermediate.

Bacteriorhodopsin (bR)[1] is a 7-helix transmembrane protein found in the purple membrane of *Halobacterium salinarium*. It functions as an electrogenic light-driven proton pump, translocating protons from the cytoplasmic to extracellular medium (Stoeckenius & Bogomolni, 1982). Although considerable information is now available about the 3-D structure and structural changes of bR during the photocycle (Grigorieff et al., 1996; Krebs & Khorana, 1993; Lanyi, 1993; Rothschild & Sonar, 1995), major features of bR are still not understood. These include the molecular basis for energy transduction, the pathway of proton transport and the fine-tuning of the visible absorption of bR and its photointermediates.

Much interest has focused on the active site in bacteriorhodopsin. Evidence indicates that this active site consists of at least three residues, Asp-85, Asp-212, and Arg-82 (Braiman et al., 1988; Grigorieff et al., 1996; Mathies et al., 1991) and possibly one or more water molecules (Beaucage & Radhakrishnan, 1993; de Groot et al., 1989; Fischer et al., 1994; Maeda et al., 1994). All of these residues are in close proximity to a protonated Schiff base which links the retinylidene chromophore to the protein through the ϵ-amino group of Lys-216 (Bayley et al., 1981; Rothschild et al., 1982). A proton is transferred during the L → M step of the bR photocycle from the Schiff base to Asp-85 and then from Asp-96 to the Schiff base during the M → N step (Bousché et al., 1991; Braiman et al., 1991; Gerwert et al., 1989; Otto et al., 1989, 1990). Since Asp-96 is located approximately 10 Å from the Schiff base (Grigorieff et al., 1996), a proton conducting pathway consisting of several hydrogen-bonded residues and/or water molecules has been postulated to span this distance which may include Thr-46, Thr-89, Tyr-185, and Asp-212 (Grigorieff et al., 1996; le Coutre et al., 1995; Mathies et al., 1991; Rothschild et al., 1993). An ejection mechanism for release of a proton from the extracellular surface also exists which involves the protonation of Asp-85 (Braiman et al., 1988) and deprotonation of Glu-204 (Richter et al., 1996).

The active site also plays a key role in determining the visible absorption of bR. In the light-adapted state, bR absorbs near 570 nm, which is red shifted approximately 100−120 nm from the visible absorption of a protonated retinylidene Schiff base (referred to as the opsin shift). Although several factors can contribute to the opsin shift, most attention has been focused on the existence of a weak counterion or complex counterion which is located near the Schiff base (de Groot et al., 1989; Honig et al., 1979; Rath et al., 1993; Rothschild et al., 1984). Recently, it has been shown that the opsin shift can be effectively modeled by the interaction of a complex counterion with a protonated retinal Schiff base compound in a 6-s-*trans* configuration (Hu et al., 1994).

In most models of the bR active site, the only charged residues believed to be in the immediate vicinity of the Schiff

† This work was supported by a grant from the NSF (MCB9419059) to K.J.R. A.N. is supported by a postdoctoral fellowship from the Wenner-Gren Center Foundation (Sweden). M.C. is supported by an NIH Molecular Biophysics Training Grant (GM08291-06). T.R. is supported by an ASSERT award from the Army Research Office (DAAH04-93-G-0375).

* Address all correspondence to this author at 590 Commonwealth Avenue, Department of Physics, Boston University, Boston, MA 02215.

‡ Both T.R. and M.C. contributed equally to this work.

§ Present address: Plant Cell Biology, Lund University, Box 7007, S-220 07 LUND, Sweden.

⊗ Abstract published in *Advance ACS Abstracts,* May 15, 1997.

[1] Abbreviations: bR, bacteriorhodopsin; FTIR, Fourier transform infrared; WT, wild-type bR.

S0006-2960(97)00287-0 CCC: $14.00

base are Asp-85, Asp-212, and Arg-82. Of these, Asp-85 appears to have the largest effect on the visible λ_{max}. For example, replacement of Asp-85 with a neutral residue or lowering the pH below 3, which causes protonation of Asp-85, produces a red shift of the visible absorption to near 615 nm (Mogi et al., 1988; Otto et al., 1990; Subramaniam et al., 1990; Turner et al., 1993; Váró & Lanyi, 1989). It has been recently established that the analogous residue in sensory rhodopsin I, Asp-76, is protonated thus accounting for the red shifted λ_{max} of 587 nm (Rath et al., 1994, 1996).

In this work, we have examined the role of Thr-89 in color regulation, photocycle kinetics, and structure of the photocycle intermediates. This residue is located one turn above Asp-85 on the C-helix and is in a good position to interact with both the Schiff base and Asp-85 (Grigorieff et al., 1996). Previously, it has been suggested that Thr-89 may participate in proton transfer from Asp-96 to the Schiff base during the M → N transition either by directly transferring a proton to the Schiff base (Mathies et al., 1991) or through other intermediate residues which are part of a hydrogen-bonded network such as Tyr-185 and Asp-212 (Rothschild et al., 1993). Our evidence shows that Thr-89 influences the properties of the *all-trans* retinylidene chromophore of light-adapted bR possibly through a direct interaction with the protonated Schiff base. Changes in the properties of the M and N chromophores are also detected along with an alteration in the hydrogen-bonding of Asp-85. The rate of proton transfer to Asp-85 from the Schiff base is also slowed, although not the reprotonation of the Schiff base. Finally, the properties of the 13-*cis* retinylidene chromophore of dark-adapted bR as well as the K and L intermediates are similar to WT indicating that Thr-89 may not interact with the chromophore in these states of bR.

MATERIALS AND METHODS

Expression of T89N and T46N/T89N. Materials. All chemical reagents were purchased from Sigma Chemical Co. (St. Louis, MO). Restriction endonucleases and nucleic-acid-modifying enzymes were purchased from Promega Corp (Madison, WI), New England BioLabs (Beverly, MA), and Stratagene Cloning Systems (La Jolla, CA). Plasmid constructs were verified by dideoxy-chain termination sequencing using a Sequenase-2 kit (U.S. Biochemical Corp, Cleveland, OH) and [^{35}S]-dATP (Amersham, Arlington Heights, IL). Oligonucleotides were synthesized on a 392 DNA Synthesizer (Applied Biosystems Inc., Foster City, CA). The procedures for restriction digestion, DNA purification, DNA ligation, agarose gel electrophoresis, *Escherichia coli* DH5α cell transformations, nucleic acid quantitation and purification, and SDS−PAGE electrophoresis have been described earlier (Sambrook et al., 1989).

Plasmid Construction, Protein Expression, and Purification. Polymerase chain reaction (PCR) based mutagenesis (Ho et al., 1989) was used to construct the substitutions Thr-89 → Asn (T89N) and the double mutant Thr-46 → Asn/Thr-89 → Asn (T46N/T89N) in the native bacterioopsin *(bop)* gene. The primers used for making the single mutations were 5′-CTACGCCATCAACACGCTCGTC-3′ for the T46N, 5′-TGGCTGTTCAACACGCCGCTG-3′ for the T89N, and the compliments for each respective primer. The double mutant T46N/T89N was made by using the plasmid with the T46N mutation as the template for PCR. The procedures for PCR and other recombinant techniques were described previously (Coleman et al., 1995; Krebs et al., 1993). WT and mutant strains were grown, and purple membrane was isolated using previously described procedures (Oesterhelt & Stoeckenius, 1974). The desired mutations in the *bop* gene were sequenced prior to and after expression, to ensure that there were no undesired base changes.

Static Visible Absorption Spectroscopy. Static absorption spectra of light and dark-adapted mutants were obtained in solution (25 mM NaPi, pH 7.0) at 23 °C using a UV−vis spectrometer (Model UV-2101, Shimadzu, Kyoto, Japan or Model HP-8453, Hewlett-Packard, Corvallis, OR). Samples were dark-adapted overnight and then light-adapted as previously described (Duñach et al., 1990b; Sonar et al., 1993). Light adaptation was performed using a Dolan-Jenner lamp (Model 4715MS-12T B10) with a long-pass 505 nm (yellow) filter (Duñach et al., 1990b; Sonar et al., 1993).

Time-Resolved Absorption Spectroscopy. As previously described (Coleman et al., 1995; Duñach et al., 1990a; Sonar et al., 1993), time-resolved difference spectra were obtained using a gated optical multichannel analyzer (Model 1420 UV-enhanced optical multichannel analyzer, Model 1460 controller; Princeton Applied Research, Princeton, NJ) and a 532 nm pulsed excitation from a Nd:YAG laser (GCR-11, Spectra Physics, Mountain View, CA). Samples with absorbances between 0.3 and 0.6 o.d. (at λ_{max}) were suspended in 25 mM NaPi buffer at pH 7.0. The data acquisition window was 10 μs. The delay times given in Figure 2 refer to the time between the laser flash and the initiation time of the data acquisition window. The laser was operated at an output power of 65 mJ/pulse with a pulse width of 30 ns. To discount the possibility of photocycling from a photointermediate, absolute absorption spectra were taken under conditions identical to the flash-induced experiments to determine the amount of M intermediate built up by the probe light. The repetition frequency of the laser was 20 Hz for WT and 3 Hz for T89N to ensure that the samples returned to the unexcited state before the next excitation. The time courses of the M intermediates were determined by integrating the difference spectra over a 20 nm range about the appropriate λ_{max} (412 ± 10 nm for WT, 390 ± 10 nm for T89N) from a set of difference spectra taken at time points ranging from 5 μs to 12.5 ms using spectral analysis software (GRAMS/32, Galactic Industries, Salem, NH). The integrated intensities of the bands were then fit with a sum of exponentials using a nonlinear curve-fitting package (PeakFit Version 4, Jandel Scientific, San Rafael, CA) to determine the M intermediate rise and decay times.

Resonance Raman Spectroscopy. Resonance Raman spectroscopy of WT and the mutants was performed using a previously described apparatus (Rath et al., 1993). For time-resolved measurements, a 250 μL sample (25 mM NaPi buffer at pH 7.0 with an absorbance of 1 o.d. at 570 nm) was placed in a quartz spinning cell of 19 mm i.d. and rotated with a time period of 22 ms. Under these conditions, the sample is exposed by the probe laser beam to periodic pulses of 1.8 μs duration every 22 ms. This prevents spectral contributions from intermediates with life-times shorter than 22 ms. Samples were excited by a cylindrically focused 514.5 nm CW laser beam (8 mW at the sample) from an Argon ion laser (Model I70−4, Coherent Inc., Palo Alto, CA). The scattered radiation was collected at a right angle

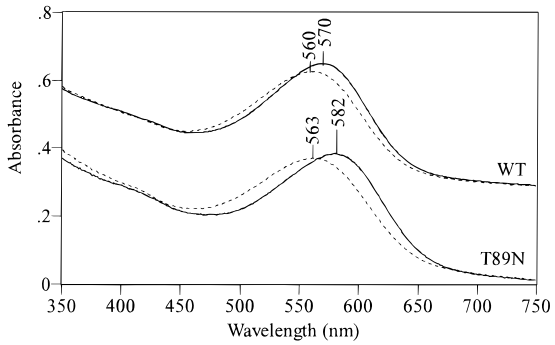

FIGURE 1: Visible absorption spectra for WT and T89N. Spectra were recorded at room temperature in pH 7.0, 25 mM NaPi buffer. Dashed lines (dark-adapted); solid lines (light-adapted). All spectra were normalized to the protein band at 285 nm. Y-scale shown is for WT dark-adapted spectrum.

to the incident laser beam and spectra were recorded at a resolution of 4 cm^{-1}. In order to achieve a low photoalteration rate, the laser power was kept below 8 mW except where indicated (Mathies et al., 1977; Rath et al., 1993). To obtain the spectrum of the M intermediate, the sample was placed in a glass capillary (Kimax, 1.5 mm i.d., Kimble Glass, Inc. Vineland, NJ) and the 457.9 nm laser line from an Argon laser was used for Raman excitation. These spectra were recorded at a resolution of 5.5 cm^{-1}. A spectrum of bR obtained under these conditions consists primarily of bands from the M intermediate. Data analysis was performed using LabCalc software (Galactic Industries, Salem, NH).

FTIR Difference Spectroscopy. Difference spectra were recorded using previously reported methods (Braiman et al., 1988; Roepe et al., 1987; Rothschild et al., 1984). Samples were prepared by air-drying approximately 100−200 $\mu g/cm^2$ of sample on a AgCl window and then rehydrating prior to insertion into a sealed transmittance cell which was mounted in a Helitran cryostat (Air Products, Allentown, PA). The water content of the sample was checked by monitoring the 3400 cm^{-1} peak. All samples, except where noted, were light-adapted at room temperature prior to cooling by illuminating the sample for at least 15 min with a 150 W tungsten light source (Dolan-Jenner Industries, Inc., Lawrence, MA) equipped with a 505 nm long-pass filter. Spectra were recorded at 2 cm^{-1} resolution using either a Nicolet Analytical Instruments 740 or 60SX spectrometer (Madison, WI).

RESULTS

Visible Absorption of T89N. Figure 1 shows the visible absorption spectrum of light and dark-adapted T89N. Compared to the λ_{max} of light-adapted WT at 570 nm, T89N is red shifted to 582 nm. In contrast, the λ_{max} of dark-adapted T89N is near 563 nm which is similar to dark-adapted WT (560 nm). This indicates that the red shift in λ_{max} of T89N is associated mainly with the light-adapted *all-trans* retinal chromophore and not the dark-adapted 13-*cis* chromophore as confirmed by FTIR difference spectroscopy (see results below).

Time-Resolved Visible Absorption. Figure 2, panels A−D, shows the visible absorption of WT (left) and T89N (right) as a function of time after a 532 nm pulse from a frequency-doubled Nd:YAG laser. Both T89N and WT form an M intermediate as indicated by the appearance of a characteristic positive band in the 390−415 nm region. However, the T89N species, which depletes after flash excitation, is red shifted approximately 15 nm relative to WT depletion in agreement with static visible absorption spectroscopy. In addition, the M intermediate formed is blue shifted over 20 nm relative to WT (390 nm vs 412 nm). As discussed below, this blue shift is confirmed by both resonance Raman and FTIR difference spectroscopy.

The T89N photocycle also includes an L intermediate; however, its decay is significantly slowed relative to WT. This can be deduced from the more prominent positive band which initially appears in the time-resolved data of T89N near 504 nm and decays as the M-like species is formed (Figure 2C). The λ_{max} of the L intermediate formed in T89N appears to be similar to WT as seen from subtractions between the early and late difference spectra shown in Figure 2 which reflect more clearly the L → M transition. An exponential fit of the integrated intensity of the M absorption band vs time (Figure 2, panels B and D) shows that the time constant for the M formation in T89N (300 μs) is much slower than WT (60 μs). In contrast, the M decay constant (3.1 ms) is similar to WT (3.0 ms).

Resonance Raman Spectroscopy. Resonance Raman spectra of bacteriorhodopsin obtained using visible excitation reflect the vibrational modes of the retinylidene chromophore (Aton et al., 1977; Braiman & Mathies, 1980; Lewis et al., 1974). As seen in Figure 3, the resonance Raman spectra (measured using a spinning cell apparatus (Argade & Rothschild, 1982) (see Materials and Methods)) of the light-adapted form of WT and T89N are similar, particularly in the configurationally sensitive C−C stretch region from 1100 to 1300 cm^{-1}. This indicates that the light-adapted T89N chromophore has predominantly an *all-trans* retinylidene configuration. However, the ethylenic C═C stretch frequency ($\nu_{C=C}$) and the Schiff base C═N stretch frequency ($\nu_{C=N}$) modes of the T89N chromophore are downshifted approximately 4 cm^{-1} relative to WT (1527 cm^{-1}, T89N; 1522 cm^{-1}, WT and 1636 cm^{-1}, T89N; 1640 cm^{-1}, WT, respectively). On the basis of the previously established linear relationship between $\nu_{C=C}$ and λ_{max} (Aton et al., 1977), the downshift of $\nu_{C=C}$ correlates with a 12 nm red shift in λ_{max} in agreement with the red shift in visible absorption of light-adapted T89N. A downshift in $\nu_{C=N}$ has also been associated with a red shift in λ_{max} (Rothschild et al., 1984) and most likely reflects a weakening of hydrogen-bonding and/or direct electrostatic interaction of the Schiff base with the Asp-85 counterion (Rath et al., 1993).

In order to examine the properties of the N-intermediate of T89N, we utilized the double mutant T46N/T89N. This mutant still exhibits the λ_{max} red shift (data not shown) and the downshift in the $\nu_{C=C}$ and $\nu_{C=N}$ modes characteristic of T89N. An increased intensity in T46N/T89N at 1185 cm^{-1} and a broadening at higher frequency of the C═C stretch mode (Figure 3) is also observed (especially at higher excitation power), which is characteristic of an accumulation of the N intermediate (Subramaniam et al., 1991). However, a similar (50 mW excitation) experiment on T89N did not result in a significant accumulation of the N intermediate (data not shown). In order to isolate contributions in the T46N/T89N spectrum from the N intermediate, an interactive subtraction was performed between spectra of T46N/T89N recorded at two different powers. As shown in Figure 3, this subtraction results in a spectrum very similar to the resonance Raman spectrum of the N intermediate in WT (Fodor et al., 1988a; Nakagawa et al., 1991). For example,

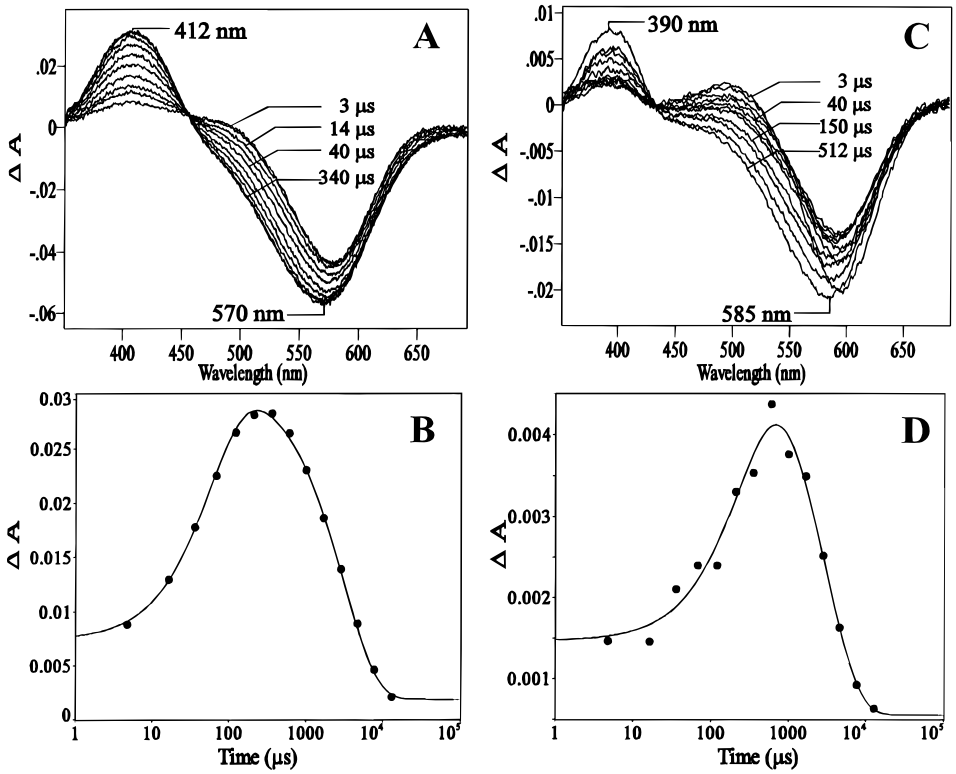

FIGURE 2: Time-resolved visible difference spectra of WT bR and T89N. Panels A and B are from WT bR and panels C and D are from T89N. Panels A and C: flash-induced difference spectra showing the rise of the M intermediate with delay times indicated. Panels B and D: Plots of integrated intensity as a function of time for the bands at 412 nm (B) and 390 nm (D).

bands appear in both spectra near 1005, 1187, 1331, 1375, and 1547 cm^{-1}. However, the major ethylenic mode which normally appears at 1530 cm^{-1} is downshifted to 1524 cm^{-1} indicative of a redshift in the λ_{max}. A downshift is also found in the Schiff base C═N stretch frequency ($\upsilon_{C=N}$) compared to the WT N intermediate (1644 vs 1638 cm^{-1}).

We also measured the resonance Raman spectra of WT, T89N, and T46N/T89N in a fixed capillary using a 457.9 nm probe wavelength which enhances the vibrational modes of the M intermediate. We find a 2−3 cm^{-1} upshift in the frequency of the band assigned to the C═C stretching mode of the M retinal chromophore of T89N relative to WT (1569 vs 1566 cm^{-1}) (Figure 4). On the basis of the linear correlation between $\upsilon_{C=C}$ and λ_{max} (Aton et al., 1977), this result further confirms that the visible absorption of the M intermediate is blue shifted relative to WT.

FTIR Difference Spectroscopy. FTIR difference spectra of T89N, T46N/T89N, and WT were recorded at 250 K using steady-state illumination (Figure 5). Under these conditions, WT exhibits spectral differences which primarily reflect the depletion of light-adapted bR (bR_{570}) and formation of the M intermediate (bR_{570} → M) (Roepe et al., 1987). For example, negative bands assigned to the vibrational modes of the light-adapted bR chromophore appear at 1640 cm^{-1} (C═N stretch of protonated Schiff base) and 1527 cm^{-1} (ethylenic C═C stretch). While positive bands which arise from the vibrational modes of the M chromophore are normally weak in the infrared, the ethylenic C═C stretching mode still appears at around 1565 cm^{-1}. In addition, protein bands appear in the carboxylic acid stretch region (1700−1800 cm^{-1}), which are assigned to protonation or hydrogen-bonding changes of specific Asp or Glu residues. These include a positive band at 1762 cm^{-1} due to the protonation of Asp-85, and negative/positive bands at 1742/1748 cm^{-1} and 1733/1726 cm^{-1} attributed to hydrogen bonding changes of Asp-96 and Asp-115, respectively (Braiman et al., 1988; Fahmy et al., 1992; Gerwert et al., 1989). A small negative shoulder near 1700 cm^{-1} has recently been assigned to the deprotonation of Glu-204 (Brown et al., 1995).

Bands assigned to the retinal chromophore in the FTIR difference spectra of T89N and T46N/T89N confirm the results obtained from resonance Raman and visible absorption spectroscopy. In particular, both T89N and T46N/T89N exhibit downshifted ethylenic C═C stretch frequencies ($\upsilon_{C=C}$) (1522 cm^{-1}, T89N; 1522 cm^{-1}, T46N/T89N; 1527 cm^{-1}, WT) and C═N stretch frequencies ($\upsilon_{C=N}$) (1634 cm^{-1}, T89N; 1634 cm^{-1} T46N/T89N; 1640 cm^{-1}, WT)[2] (Figure 5) consistent with a 12 nm red shift in the λ_{max} of the light adapted form of these mutants. The upshift of the C═C stretch of the M intermediate ($\upsilon_{C=C}$) (1565 $cm^{-1,}$ WT; 1567 cm^{-1}, T89N) supports the conclusion that this intermediate has a blue-shifted λ_{max}.

In the case of protein assigned bands, several changes were found in the carboxyl (C═O) stretch region (Figure 5). First, the positive band at 1762 cm^{-1} assigned to Asp-85 is absent in the T89N bR → M difference spectrum. Instead, a new band is found near 1752 cm^{-1} which appears to be superimposed on the 1748/1742 cm^{-1} bands assigned to Asp-96. This is confirmed in the bR → M difference spectrum of the double mutant T46N/T89N where the bands due to Asp-96 are absent as a result of the T46N substitution (Coleman, M., Russell, T. S., Nilsson, A., & Rothschild, K. J., unpublished data). Thus, we conclude that the C═O stretching frequency of Asp-85 downshifts by approximately

[2] The increased intensity of the positive band near 1648 cm^{-1} is most likely due to the reduced overlap between this band and the C═N stretch mode compared to WT.

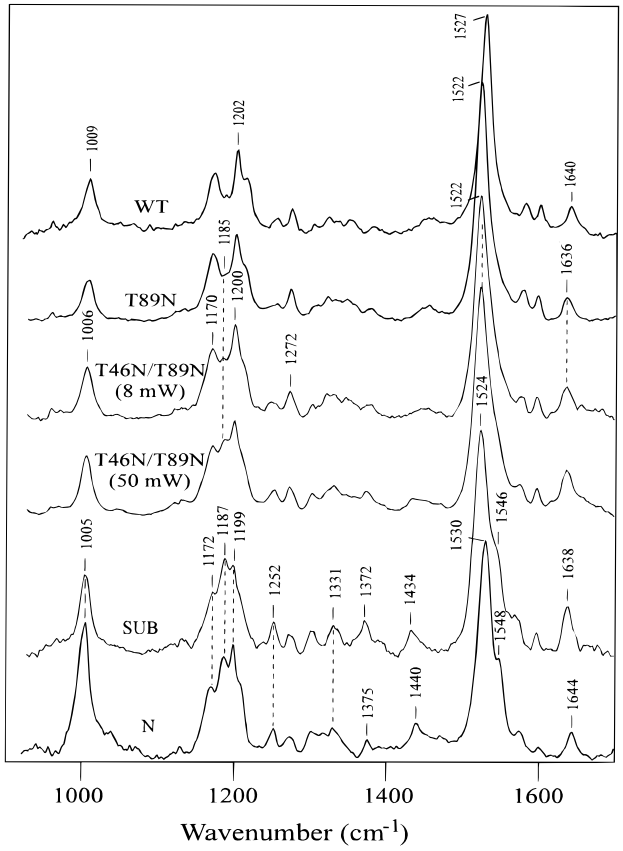

FIGURE 3: Resonance Raman spectra of WT and T89N. Spectra were recorded with 514.5 nm laser excitation using a spinning-cell apparatus (see Materials and Methods). The SUB spectrum refers to the N intermediate of T46N/T489N obtained by interactively subtracting the low-power (8 mW) excitation spectrum from the high-power (50 mW) spectrum. The subtraction factor was chosen so as not to produce any negative bands. The N intermediate of WT was obtained as reported elsewhere (Subramaniam et al., 1991).

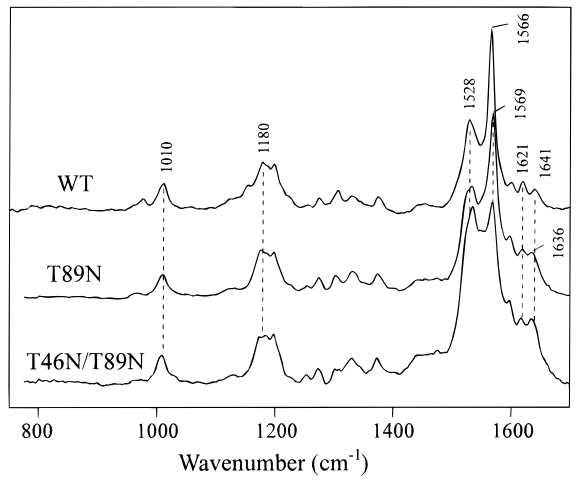

FIGURE 4: Resonance Raman spectra of WT and T89N. Samples were in a fixed capillary and spectra were recorded with 457.9 laser excitation (10 mW at sample) which enhances vibrations from the M intermediate.

10 cm^{-1} due to the Thr-89 → Asn substitution in the M intermediate. The Asp-85 C═O stretch mode in the bR → N difference spectrum of T46N/T89N (Figure 5, dashed line) is also downshifted from its normal frequency at 1755 cm^{-1} in WT (Ludlam et al., 1995) to 1746 cm^{-1}.[3]

The bR → K FTIR difference spectrum of T89N was measured from both fully light-adapted and dark-adapted

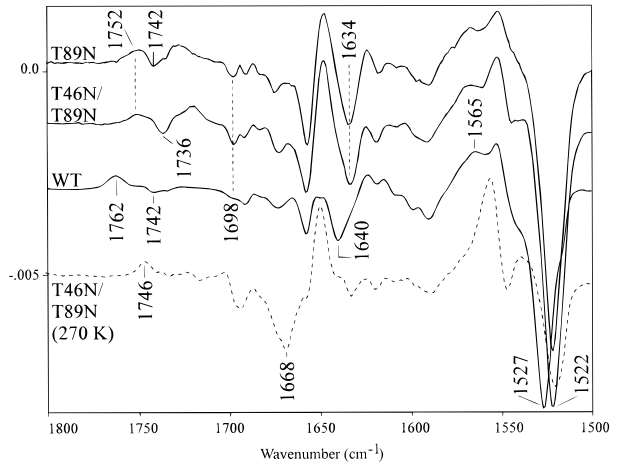

FIGURE 5: bR → M FTIR difference spectra of T89N, T46N/T89N, and WT. Spectra were recorded at 250 K using steady state illumination. The bR → N FTIR difference spectrum of T46N/T89N, was recorded at 270 K (dashed line). Y-scale shown is for T89N difference spectrum (see Materials and Methods).

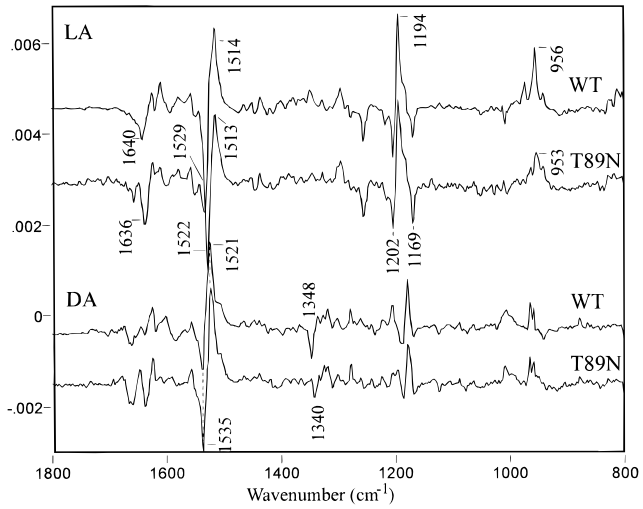

FIGURE 6: FTIR bR → K difference spectra of T89N and WT. Difference spectra were recorded at 81 K for both light-adapted (top pair) and dark-adapted (bottom pair) conditions. Note that the dark-adapted WT spectrum (but not the T89N spectrum) shown was computed by interactively subtracting a light-adapted from a dark-adapted bR → K difference spectrum which results in a difference spectrum for the 13-*cis* retinal containing species of dark-adapted WT (Roepe et al., 1988) (see Materials and Methods).

samples (Figure 6). The light-adapted bR → K spectrum of T89N is similar to WT except for the downshift in the frequency C═C and C═N stretch modes of the chromophore from 1529 and 1640 cm^{-1} to 1522 and 1636 cm^{-1}, respectively, in agreement with the bR → M difference spectrum. We also find a downshift of the hydrogen-out-of-plane (HOOP) mode (∼3 cm^{-1}) relative to WT, although less than T89A and T89D (∼7 cm^{-1}) (Rothschild et al., 1992). In contrast, the C═C and C═N stretching modes of the chromophore in the dark-adapted bR → K difference spectrum of T89N showed smaller shifts of only 1 cm^{-1} when compared to the 13-*cis* component in dark-adapted WT (Roepe et al., 1988). This confirms the results from UV−vis spectroscopy that this component of dark-adapted bR is

[3] A negative band at 1742 cm^{-1} due to Asp-96 deprotonation is downshifted due to the single T46N substitution (Coleman, M., Russell, T. S., Nilsson, A., & Rothschild, K. J., unpublished data).

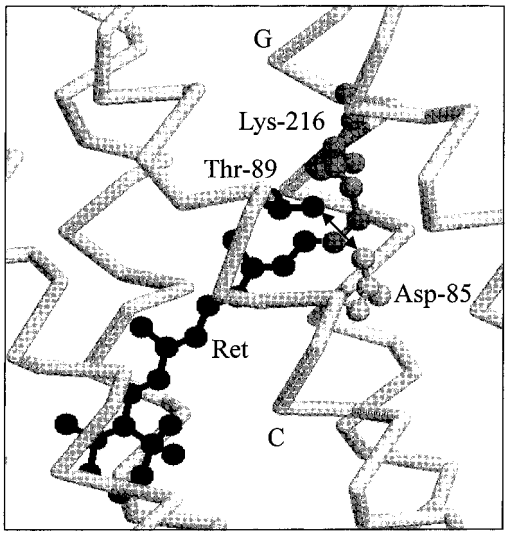

FIGURE 7: Structural model of bR from electron diffraction derived coordinates. A number of key residues in the retinal binding pocket are shown (Thr-89 and Asp-85 on the C helix and Lys-216 on the G helix) (Grigorieff et al., 1996). Arrow shows distance (3.1 Å) between the oxygen from the Thr-89 hydroxyl group and the nearest oxygen of the Asp-85 carboxylate group. Ret denotes the *all-trans* retinylidene chromophore.

not significantly altered. Interestingly, this spectrum displayed no contributions from the *all-trans* retinal component which is normally present in the dark-adapted WT spectrum.[4] This indicates that dark-adapted T89N exists (at least at low temperature) in an almost completely 13-*cis* configuration. Finally, we find that the bR → K difference spectra for both light and dark-adapted T89N and WT are very similar including the $\upsilon_{C=C}$ of the K intermediates (positive bands at 1513 and 1521 cm^{-1}, Figure 6). This indicates that unlike light-adapted T89N, the chromophore of the K species does not undergo a significant λ_{max} shift.

DISCUSSION

In this work, we have examined the role of Thr-89 in the structure and function of bacteriorhodopsin. Thr-89 is located one turn above the Asp-85 counterion on the C-helix. In a refined 3-D model of bacteriorhodopsin based on electron diffraction (Grigorieff et al., 1996), the hydroxyl oxygen of Thr-89 was found to be located 3.1 Å from the oxygen on the side-chain of Asp-85, 2.9 Å from the backbone carbonyl oxygen of Asp-85, and 3.8 Å from the nitrogen of the Schiff base (Figure 7). Thus, Thr-89 is in a good position to participate directly in the active site of bR and to interact indirectly with other residues in the retinal binding pocket.

As discussed below, our results indicate that Thr-89 exerts a significant influence on the properties of the retinal chromophore in light-adapted bR. Changes are also found in the chromophore and protein structure of the M and N intermediates as well as on the ability of the Schiff base to transfer a proton to Asp-85 during formation of the M intermediate. In contrast, Thr-89 did not appear to influence the properties of the 13-*cis* chromophores of dark-adapted bR and the K and L intermediates.

(1) Thr-89 Is Involved in Color Regulation of Light-Adapted Bacteriorhodopsin. The T89N and T46N/T89N substitutions produced a significant red shift of the λ_{max} of the light-adapted state of bacteriorhodopsin from 570 to 582 nm. An earlier study also indicated that two other single substitutions at the Thr-89 position, Asp and Ala, produce red shifted chromophores as based on shifts in the $\upsilon_{C=C}$ stretch frequency (Rothschild et al., 1992). Furthermore, these effects do not appear to involve a significant change in the structure of the *all-trans* retinal since the frequency of the C−C stretch bands in the structurally sensitive fingerprint region of the chromophore are largely unaffected. Instead, the shift in C=N stretching frequency of the Schiff base indicates that the red shift arises from a change in the immediate vicinity of the protonated Schiff base. Such a red shift could occur, for example, if a favorable interaction between the positive charge on the protonated Schiff base nitrogen and the partial negative oxygen on the Thr is lost due to substitutions at this position. Alternatively, increased protonation of Asp-212, which is located near Thr-89, or alterations in a water molecule in this region could also produce a λ_{max} shift (Rath et al., 1993; Rothschild et al., 1992). Interestingly, it has previously been suggested on the basis of sequence homology that, in addition to charged amino acid residues such as Asp, Glu, and Arg, hydroxyl-containing residues such as Tyr, Thr, and Ser also play a role in color regulation of retinal pigments including the visual rhodopsins; although most changes observed are blue shifts (Yokoyama, 1995).

(2) The T89N Substitution Alters the M and N Intermediates of the bR Photocycle. Similar to light adapted T89N, we found that the M and N intermediates of the T89N photocycle, which contain 13-*cis* chromophores with unprotonated and protonated Schiff bases, respectively, have altered chromophores. In the case of the M intermediate, the λ_{max} exhibits a blue shift of approximately 20 nm toward the normal λ_{max} of unprotonated Schiff base retinylidene compounds, whereas the N intermediate λ_{max} is red shifted similar to light-adapted T89N. One explanation is that these λ_{max} shifts reflect the loss of an interaction which normally exists between Thr-89 and the chromophore for the M and N intermediates. A perturbation in the Asp-85 carboxylic acid group of the M and N intermediates is also detected which may be related to the λ_{max} shifts of these intermediates as well as to the slowed transfer of a proton from the Schiff base to Asp-85 during the L → M transition.

In contrast, the λ_{max} of the 13-*cis*/C=N *syn* species (Harbison et al., 1984) present in dark-adapted T89N is much less affected by the Thr-89 → Asn substitution. The same conclusion was reached for the K and L species of the light-adapted photocycle, which contain 13-cis/C=N *anti* chromophores (Braiman & Mathies, 1982; Fodor et al., 1988b). One possible explanation is that unlike in light-adapted bR, Thr-89 may not interact strongly with the protonated Schiff base in these species. In general, any chromophore isomerization or protein conformational change which removes Thr-89 from the immediate vicinity of this bond should have the effect of minimizing the influence of Thr-89 on the λ_{max}. Overall, these results may reflect a pattern of structural changes in the active site. The initial *all-trans* to 13-*cis* chromophore isomerization during the bR → K transition

[4] If dark-adapted T89N is completely 13-*cis* at room temperature, the λ_{max} of this form should be compared to the pure 13-*cis* component of dark-adapted WT. This would imply a λ_{max} red shift similar to the light-adapted form. However, the good agreement between the C=C stretch frequency of the 13-*cis* components of WT and T89N is still a strong indication that the λ_{max} is not significantly shifted.

removes the interaction of Thr-89 with the Schiff base. It is also absent in the L intermediate and then re-established in the M and N intermediates.

(3) T89N Influences Proton Transfer during the L → M but Not the M → N Transition. It has been previously established that a proton is transferred from the Schiff base to Asp-85 during the L → M transition (Braiman et al., 1988) and from Asp-96 to the Schiff base during M → N (Bousché et al., 1991; Braiman et al.; 1991, Gerwert et al., 1989; Otto et al., 1989, 1990). We find that the T89N substitution affects primarily the L → M transition, slowing it approximately 3−5-fold relative to WT bR. In contrast, the kinetics of the M → N transition are almost identical to WT. A simple explanation for these effects is that the interaction of Thr-89 with the Schiff base and Asp-85 influences the L → M transition by altering the relative position of these groups during proton transfer. A change in the interaction of these groups upon M formation is also indicated by the perturbation in the Asp-85 carboxylic acid group. In contrast, the same substitution does not appear to affect the transfer of a proton from Asp-96 to the Schiff base. Although this implies that Thr-89 does not participate in a proton transporting wire that conducts a proton from Asp-96 to the Schiff base (Mathies et al., 1991; Rothschild et al., 1992, 1993), the possibility that a water molecule substitutes for Thr-89 in such a pathway cannot be eliminated.

In conclusion, this work demonstrates that Thr-89 participates in the bR active site through interactions with the Schiff base and/or Asp-85. In order to better define the nature of these interactions, future studies might utilize methods which do not perturb the system as significantly as site-directed mutagenesis. One possibility is the use of site-directed isotope labeling which enables an isotope to be incorporated at any position in the bR structure (Sonar et al., 1994). When combined with spectroscopic approaches such as FTIR difference spectroscopy and solid-state NMR, this approach provides specific information about the structure and structural changes of specific side-chains in an unperturbed protein.

ACKNOWLEDGMENT

We wish to thank Xiao-Mei Liu and Drs. J. Olejnik, S. Williams, and L. Smilowitz for helpful discussions.

REFERENCES

Argade, P. V., & Rothschild, K. J. (1982) *Methods Enzymol. 88*, 643−648.

Aton, B., Doukas, A. G., Callender, R. H., Becher, B., & Ebrey, T. G. (1977) *Biochemistry 16*, 2995−2999.

Bayley, H., Huang, K.-S., Radhakrishnan, R., Ross, A. H., Takagaki, Y., & Khorana, H. G. (1981) *Proc. Natl. Acad. Sci. U.S.A. 78*, 2225−2229.

Beaucage, S. L., & Radhakrishnan, P. I. (1993) *Tetrahedron 49*, 1925−1963.

Bousché, O., Braiman, M., He, Y. W., Marti, T., Khorana, H. G., & Rothschild, K. J. (1991) *J. Biol. Chem. 266*, 11063−11067.

Braiman, M., & Mathies, R. (1980) *Biochemistry 19*, 5421−5428.

Braiman, M., & Mathies, R. (1982) *Proc. Natl. Acad. Sci. U.S.A. 79*, 403−407.

Braiman, M. S., Mogi, T., Marti, T., Stern, L. J., Khorana, H. G., & Rothschild, K. J. (1988) *Biochemistry 27*, 8516−8520.

Braiman, M. S., Bousché, O., & Rothschild, K. J. (1991) *Proc. Natl. Acad. Sci. U.S.A. 88*, 2388−2392.

Brown, L. S., Sasaki, J., Kandori, H., Maeda, A., Needleman, R., & Lanyi, J. K. (1995) *J. Biol. Chem. 270*, 27122−27126.

Coleman, M., Nilsson, A., Russell, T. S., Rath, P., Pandey, R., & Rothschild, K. J. (1995) *Biochemistry 34*, 15599−15606.

de Groot, H. J. M., Harbison, G. S., Herzfeld, J., & Griffin, R. G. (1989) *Biochemistry 28*, 3346−3353.

Duñach, M., Berkowitz, S., Marti, T., He, Y. W., Subramaniam, S., Khorana, H. G., & Rothschild, K. J. (1990a) *J. Biol. Chem. 265*, 16978−16984.

Duñach, M., Marti, T., Khorana, H. G., & Rothschild, K. J. (1990b) *Proc. Natl. Acad. Sci. U.S.A. 87*, 9873−9877.

Fahmy, K., Weidlich, O., Engelhard, M., Tittor, J., Oesterhelt, D., & Siebert, F. (1992) *Photochem. Photobiol. 56*, 1073−1083.

Fischer, W., Sonar, S., Marti, T., Khorana, H. G., & Rothschild, K. J. (1994) *Biochemistry 33*, 12757−12762.

Fodor, S. P. A., Ames, J. B., Gebhard, R., Van den Berg, E. M. M., Stoeckenius, W., Lugtenburg, J., & Mathies, R. A. (1988a) *Biochemistry 27*, 7097−7101.

Fodor, S. P. A., Pollard, W. T., Gebhard, R., Van den Berg, E. M. M., Lugtenburg, J., & Mathies, R. A. (1988b) *Proc. Natl. Acad. Sci. U.S.A. 85*, 2156−2160.

Gerwert, K., Hess, B., Soppa, J., & Oesterhelt, D. (1989) *Proc. Natl. Acad. Sci. U.S.A. 86*, 4943−4947.

Grigorieff, N., Ceska, T. A., Downing, K. H., Baldwin, J. M., & Henderson, R. (1996) *J. Mol. Biol. 259*, 393−421.

Harbison, G. S., Smith, S. O., Pardoen, J. A., Winkel, C., Lugtenburg, J., Herzfeld, J., Mathies, R., & Griffin, R. G. (1984) *Proc. Natl. Acad. Sci. U.S.A. 81*, 1706−1709.

Ho, S. N., Hunt, H. D., Horton, R. M., Pullen, J. K., & Pease, L. R. (1989) *Gene 77*, 51−69.

Honig, B., Dinur, U., Nakanishi, K., Balogh-Nair, V., Gawinowicz, M. A., Arnaboldi, M., & Motto, M. G. (1979) *J. Am. Chem. Soc. 101*, 7084−7086.

Hu, J., Griffin, R. G., & Herzfeld, J. (1994) *Proc. Natl. Acad. Sci. U.S.A. 91*, 8880−8884.

Krebs, M. P., & Khorana, H. G. (1993) *J. Bacteriol. 175*, 1555−1558.

Krebs, M. P., Mollaaghababa, R., & Khorana, H. G. (1993) *Proc. Natl. Acad. Sci. U.S.A. 90*, 1987−1991.

Lanyi, J. K. (1993) *Biochim. Biophys. Acta 1183*, 241−261.

le Coutre, J., Tittor, J., Oesterhelt, D., & Gerwert, K. (1995) *Proc. Natl. Acad. Sci. U.S.A. 92*, 4962−4966.

Lewis, A., Spoonhower, J., Bogomolni, R. A., Lozier, R. H., & Stoeckenius, W. (1974) *Proc. Natl. Acad. Sci. U.S.A. 71*, 4462−4466.

Ludlam, C. F. C., Sonar, S., Lee, C.-P., Coleman, M., Herzfeld, J., RajBhandary, U. L., & Rothschild, K. J. (1995) *Biochemistry 34*, 2−6.

Maeda, A., Sasaki, J., Yamazaki, Y., Needleman, R., & Lanyi, J. K. (1994) *Biochemistry 33*, 1713−1717.

Mathies, R., Freedman, T. B., & Stryer, L. (1977) *J. Mol. Biol. 109*, 367−372.

Mathies, R. A., Lin, S. W., Ames, J. B., & Pollard, W. T. (1991) *Annu. Rev. Biophys. Biophys. Chem. 20*, 491−518.

Mogi, T., Stern, L. J., Marti, T., Chao, B. H., & Khorana, H. G. (1988) *Proc. Natl. Acad. Sci. U.S.A. 85*, 4148−4152.

Nakagawa, M., Maeda, A., Ogura, T., & Kitagawa, T. (1991) *J. Mol. Struct. 242*, 221−234.

Oesterhelt, D., & Stoeckenius, W. (1974) *Methods Enzymol. 31*, 667−678.

Otto, H., Marti, T., Holz, M., Mogi, T., Lindau, M., Khorana, H. G., & Heyn, M. P. (1989) *Proc. Natl. Acad. Sci. U.S.A. 86*, 9228−9232.

Otto, H., Marti, T., Holz, M., Mogi, T., Stern, L. J., Engel, F., Khorana, H. G., & Heyn, M. P. (1990) *Proc. Natl. Acad. Sci. U.S.A. 87*, 1018−1022.

Rath, P., Marti, T., Sonar, S., Khorana, H. G., & Rothschild, K. J. (1993) *J. Biol. Chem. 268*, 17742−17749.

Rath, P., Olson, K. D., Spudich, J. L., & Rothschild, K. J. (1994) *Biochemistry 33*, 5600−5606.

Rath, P., Spudich, E., Neal, D. D., Spudich, J. L., & Rothschild, K. J. (1996) *Biochemistry 35*, 6690−6696.

Richter, H.-T., Brown, L. S., Needleman, R., & Lanyi, J. K. (1996) *Biochemistry 35*, 4054−4062.

Roepe, P., Ahl, P. L., Das Gupta, S. K., Herzfeld, J., & Rothschild, K. J. (1987) *Biochemistry 26*, 6696−6707.

Roepe, P. D., Ahl, P. L., Herzfeld, J., Lugtenburg, J., & Rothschild, K. J. (1988) *J. Biol. Chem. 263*, 5110−5117.

Rothschild, K. J., Argade, P. V., Earnest, T. N., Huang, K. S., London, E., Liao, M. J., Bayley, H., Khorana, H. G., & Herzfeld, J. (1982) *J. Biol. Chem. 257*, 8592−8595.

Rothschild, K. J., Roepe, P., Lugtenburg, J., & Pardoen, J. A. (1984) *Biochemistry 23*, 6103−6109.

Rothschild, K. J., He, Y. W., Sonar, S., Marti, T., & Khorana, H. G. (1992) *J. Biol. Chem. 267*, 1615−1622.

Rothschild, K. J., Marti, T., Sonar, S., He, Y. W., Rath, P., Fischer, W., Bousché, O., & Khorana, H. (1993) *J. Biol. Chem. 268*, 27046−27052.

Rothschild, K. J., & Sonar, S. (1995) in *CRC handbook of organic photochemistry and photobiology* (Horspool, W. M., & Song, P.-S., Eds.) pp 1521−1544, CRC Press, Inc., London.

Sambrook, J., Fritsch, E. F., & Maniatis, T. (1989) *Molecular cloning: a laboratory manual*, 2nd ed., Cold Spring Harbor Lab., Cold Spring Harbor, NY.

Sonar, S., Krebs, M. P., Khorana, H. G., & Rothschild, K. J. (1993) *Biochemistry 32*, 2263−2271.

Sonar, S., Lee, C. P., Coleman, M., Patel, N., Liu, X., Marti, T., Khorana, H. G., Rajbhandary, U. L., & Rothschild, K. (1994) *Struct. Biol. 1*, 512−517.

Stoeckenius, W., & Bogomolni, R. A. (1982) *Annu. Rev. Biochem. 51*, 587−616.

Subramaniam, S., Marti, T., & Khorana, H. G. (1990) *Proc. Natl. Acad. Sci. U.S.A. 87*, 1013−1017.

Subramaniam, S., Greenhalgh, D. A., Rath, P., Rothschild, K. J., & Khorana, H. G. (1991) *Proc. Natl. Acad. Sci. U.S.A. 88*, 6873−6877.

Turner, G. J., Miercke, L. W., Thorgeirsson, T. E., Kilger, D., Betlach, M. C., & Stroud, R. M. (1993) *Biochemistry 32*, 1332−1337.

Váró, G., & Lanyi, J. K. (1989) *Biophys. J. 56*, 1143−1151.

Yokoyama, S. (1995) *Mol. Biol. Evol. 12*, 53−61.

BI970287L